Pulsed Laser Ablation Synthesis of ZnO Nanoparticles and Enhanced Cytotoxicity on Ocular Melanoma Cells via Combined Femtosecond Laser Treatment

Khalid T. Nawaf
Laser Institute for Research and Applications (LIRA), Beni-Suef University, Egypt | Anbar Health Department, Anbar Province, Ministry of Health, Iraq
khalid_nawaf76@lira.bsu.edu.eg

Safaa Taha
Laser Institute for Research and Applications (LIRA), Beni-Suef University, Egypt
safaatahamawd6@lira.bsu.edu.eg

Yasmin Abd El-Salam
Laser Institute for Research and Applications (LIRA), Beni-Suef University, Egypt
yasmena@lira.bsu.edu.eg

Fatma Abdel Samad
Laser Institute for Research and Applications (LIRA), Beni-Suef University, Egypt
fatmaabdalsamad@lira.bsu.edu.eg

Hala M. Rifaat
Microbial Chemistry Department, National Research Centre, Dokki, Giza, Egypt
halamohamed23@yahoo.com

Ahmed O. El-Gendy
Department of Microbiology and Immunology, Faculty of Pharmacy, Beni-Suef University, Egypt | Laser Institute for Research and Applications (LIRA), Beni-Suef University, Beni-Suef, Egypt
ahmed.elgendy@pharm.bsu.edu.eg (corresponding author)

Tarek Mohamed
Laser Institute for Research and Applications (LIRA), Beni-Suef University, Beni-Suef, Egypt | Department of Engineering, Faculty of Advanced Technology and Multidiscipline, Universitas Airlangga, Indonesia
tarek_mohamed1969@lira.bsu.edu.eg

Received: 30 May 2025 | Revised: 12 July 2025 and 16 July 2025 | Accepted: 20 July 2025

 DOI: https://doi.org/10.48084/etasr.12452

ABSTRACT

Ocular melanoma, a malignant tumor that arises from the uveal tract, presents significant therapeutic challenges due to its intricate anatomy and limited accessibility. Recent advances propose a novel targeted treatment approach by combining femtosecond laser technology with Zinc Oxide Nanoparticles (ZnO-NPs) synthesized through laser ablation. This study investigates the combined effects of femtosecond laser irradiation and ZnO-NPs on A375 melanoma cells. ZnO-NPs were synthesized by ablating high-purity zinc in distilled water using a 532 nm Nd:YAG laser. The nanoparticles were characterized using UV-Vis

spectroscopy, TEM, EDX, and concentration analysis, revealing optimal size distribution and surface properties suitable for biological applications. A375 ocular melanoma cells were treated with ZnO-NPs, followed by femtosecond laser irradiation at wavelengths of 420 and 700 nm. Cytotoxicity was assessed using MTT assays, which showed that the combination of ZnO-NPs and 420 nm laser irradiation significantly reduced cell viability compared to either treatment alone. This innovative approach underscores the potential of combining nanotechnology with femtosecond laser technology to achieve precise and effective cancer cell targeting. Further in vivo studies are required to evaluate the clinical applicability of this promising strategy.

Keywords-ocular melanoma; femtosecond laser-based treatment; Zinc oxide nanoparticles (ZnO-NPs); laser ablation synthesis technique; Photodynamic Therapy (PDT)

I. INTRODUCTION

In recent years, the occurrence of malignancies has increased steadily, with carcinogenesis increasingly affecting younger populations [1]. Melanoma is a kind of cancer that develops from melanocytes, which are cells in the skin's epidermis that produce color [2-4]. Early-stage melanoma is highly treatable with appropriate treatments. However, metastatic melanoma has a poor prognosis and is difficult to treat. As a result, the life expectancy of patients with metastatic melanoma is significantly reduced, ranging from 4.7 to 11 months [5]. Surgery is usually the main treatment for melanoma, which aims to remove the affected skin and is often combined with chemotherapy and radiation therapy. This procedure is also utilized for patients with limited metastases to address isolated areas of carcinoma [6]. Malignant melanoma cells pose significant treatment challenges with existing chemotherapeutic drugs due to their inherent drug resistance, which severely reduces the survival rates of affected patients. Furthermore, these medications have several adverse effects [7]. Advances such as immunotherapy and molecular targeting therapy have improved outcomes for many patients, but unfortunately, these treatments are not effective for everyone [8].

Therefore, it is crucial to develop alternative treatments that can selectively target and destroy malignant melanoma cells while minimizing damage to surrounding healthy tissues. Recently, rapid advances in nanotechnology have shown promise in cancer treatment. Nanoparticles (NPs) have garnered significant interest in chemotherapy due to their superior bioavailability, solubility, biocompatibility, and multifunctionality compared to conventional chemotherapeutic agents [9]. Zinc Oxide NPs (ZnO-NPs) are highly versatile due to their potential for use in solar cells [10], varistors [11], gas sensors [12], piezoelectric devices, transducers, chemical absorbent [13], sun-screens, UV absorbers [14], UV light-emitting devices [15] and electrostatic dissipative coating [16]. ZnO-NPs are versatile nanomaterials characterized by their exceptional properties, such as remarkable chemical and physical stability, biocompatibility, and size-dependent functionality [17, 18]. These characteristics make ZnO-NPs highly effective for various biomedical applications, particularly cancer treatment [19]. ZnO-NPs, due to their semiconductor properties and distinctive surface characteristics, demonstrate cytotoxic effects against cancer cells. These effects are predominantly driven by the generation of Reactive Oxygen Species (ROS), which are instrumental in triggering oxidative stress [20].

Recently, some physical and chemical techniques have been studied for the liquid-phase formation of ZnO-NPs, such as hydrothermal methods [21], thermal plasma [22], sol-gel [23], and Pulsed Laser Ablation in Liquids (PLAL) [24, 25]. Laser Ablation in Liquid (LAL) involves directing a laser pulse at a solid target submerged in a liquid, causing the ejection of material and the formation of nanostructures. The interaction between laser and matter is significantly influenced by the irradiance and pulse duration [26]. Knowing the consequences of the PLAL parameters, liquid medium, wavelength, fluence, and irradiation period, is necessary for the controlled synthesis of NPs to create crucial physical qualities for energy usage, such as particle size and structure [27].

This study aimed to evaluate the cytotoxicity and anticancer potential of ZnO-NPs synthesized by PLAL in conjunction with femtosecond laser treatment on the human melanoma cell line (A375).

II. MATERIALS AND METHODS

A. Synthesis of ZnO-NPs

Figure 1 demonstrates the design of the experiment for creating ZnO-NPs in liquid using PLAL. A Q-switched Nd:YAG laser (Quanta-Ray PRO-Series 350–10, Spectra-Physics) was utilized to ablate the Zn bulk target. This system delivers pulses with a maximum energy of 1400 mJ per pulse, operating at a wavelength of 532 nm, a repetition rate of 10 Hz, and a pulse duration of 10 ns. Before the ablation procedure, the zinc surface with a purity of approximately 99.99% was thoroughly cleaned with alcohol, ultrasonicated, and polished to ensure smoothness and reduce beam scattering during the ablation procedure. After being secured in a holder, the zinc target was submerged in a beaker containing 10 ml of distilled water. As shown in Figure 1, a convex lens with a focal length of 100 mm was employed to focus the laser beam onto the Zn target after it had been directed to it by three highly reflective mirrors.

To enhance nanoparticle formation and prevent aggregation, a motorized sample spinner was used to uniformly distribute the laser beam across the zinc surface, ensuring consistent laser exposure and minimizing power loss. In this research, ZnO-NP colloids were created at variable Laser Ablation Times (LATs) of 5, 10, 15, and 20 min at a constant average power of 200 mW. In addition, some measurements such as absorption, particle size, concentration, and Energy Dispersive X-ray (EDX) were performed.

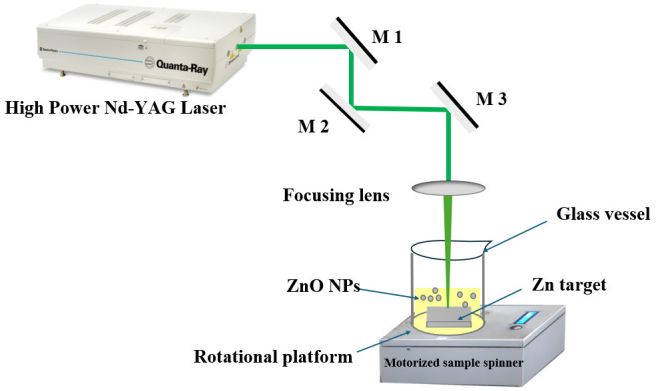

Fig. 1. Experimental setup of PLA for generation of ZnO-NPs colloids utilizing a 532 nm pulsed Nd: YAG laser.

B. Cell Culture and Cytotoxicity Assay

In a humidified environment with 5% CO_2, the human malignant melanoma A375 cell line (ATCC® CRL-1619™) was cultured at 37°C in preheated DMEM (Biowest) supplemented with 10% fetal bovine serum (Gibco, USA) and 1% penicillin-streptomycin to maintain optimal growth conditions. Subculturing was performed when cells reached 80-90% confluence, as confirmed under an inverted fluorescence microscope (Leica DMi8).

A375 cells were seeded at a density of 10,000 cells per well in 96-well plates for the tests. After a 24-hour incubation period, cells were treated with various concentrations of ZnO-NPs synthesized by laser ablation. ZnO-NPs were added to the wells at final concentrations of 15.3, 7.65, 3.82, 1.91, 0.9, and 0.47 µg/mL. In separate groups, some wells were subjected to femtosecond laser treatment at wavelengths of 700 nm or 420 nm, either with or without the presence of ZnO-NPs. For the laser treatment groups involving ZnO-NPs, the NP concentration was fixed at 15.3 µg/mL. An MTT assay was conducted on all wells, including a control group that did not receive treatment with ZnO-NPs or femtosecond laser exposure.

C. Femtosecond Laser System Setup and Cytotoxicity Assessment Using MTT Assay

The effect of tunable femtosecond laser light on the human malignant melanoma A375 cell line was studied using a mode-locked femtosecond Ti:sapphire MAI TAI HP laser (Spectra-Physics). This laser operated with an average power of 1.5-2.9 W, a repetition rate of 80 MHz, and a wavelength range of 690-1040 nm, producing pulses for the INSPIRE HF100 laser system (Spectra-Physics). A notable feature of the INSPIRE HF100 system is its ability to adjust the wavelength, allowing for precise customization of experimental conditions. In addition to the standard infrared pump wavelengths, the system can also function in OPO or SHG modes. When the Ti:sapphire laser is tuned and the potassium dihydrogen phosphate (KDP) second harmonic nonlinear crystal is rotated, the SHG mode produces output within a wavelength range of 345-520 nm. Simultaneously, the OPO mode generates a signal between 490-750 nm and an idler between 930-2500 nm by tuning Lithium Niobate (LN) crystals.

These capabilities allow for wavelength adjustment from 345 to 2500 nm, output through four exit apertures. The power of the laser beam was measured using a Newport 843R power meter. As shown in Figure 2, the laser beam was positioned approximately 10 cm above each well in a covered 96-well plate, ensuring that the cells remained free from ambient contamination during irradiation. The initial laser beam diameter of ~2 mm was expanded to ~20 mm using a beam expander composed of two converging lenses. An adjustable iris was used to modify the laser beam's diameter, while a laser beam attenuator controlled the intensity directed at the cells. The laser beam was focused on the cells using highly reflective mirrors, as illustrated in Figure 2. The femtosecond laser light was delivered to the cells at specific wavelengths of 420 and 700 nm. The actual power reaching the cells was measured using the Newport 843R power meter. Due to a 14% loss of laser power during transmission through the 96-well plate cover, only 100 mW of laser power was effectively delivered to the cells, requiring 114-116 mW of irradiation power.

To evaluate the influence of ZnO-NP treatment and femtosecond laser irradiation on cell proliferation, the 3-[4,5-dimethylthiazol-2-yl]-2,5-diphenyl tetrazolium bromide (MTT) assay was used. This assay relies on the reduction of the yellow MTT dye by mitochondrial enzymes in viable cells, forming purple formazan crystals. This process correlates total mitochondrial activity with the number of viable cells, making it a standard method for assessing cell growth in vitro. After dissolving MTT powder (Life Technologies Corporation, M6494) in PBS, a 5 mg/mL stock solution was created and kept out of direct sunlight at 4°C. An MTT working solution (made by diluting the stock solution with DMEM in a 1:10 ratio) was applied to each well after the culture medium had been removed after a 24-hour laser irradiation. The plates were then incubated at 37°C for three hours to facilitate formazan crystal formation.

After incubation, the MTT-containing media were removed, and the plates were agitated for 12 minutes. To dissolve the formazan crystals, 100 µL of DMSO was added to each well, followed by a 15-minute incubation in a CO_2 incubator. Finally, absorbance at 570 nm was measured using an ELISA reader after the plates were agitated for three minutes on a plate shaker.

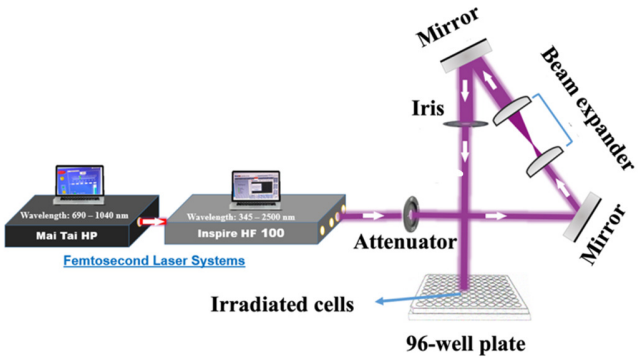

Fig. 2. Schematic illustration of the A375 cell irradiation experimental setup.

D. Statistical Analysis

The information was displayed as means ± standard errors of the means (SEMs). The study employed Tukey's multiple comparisons test and one-way analysis of variance (ANOVA) in GraphPad Prism (version 5). The criterion for statistical significance was set at $p<0.05$.

III. RESULTS AND DISCUSSION

A. Optical Characteristics

An ultraviolet-visible spectrum of ZnO-NPs colloidal solution absorbance was captured by a UV-Visible spectrophotometer (Peak Instruments C-7200, Inchinnan, UK) in the range of 190 to 1100 nm using a quartz cuvette. Figure 3 shows standard absorption spectra of the colloidal suspension, obtained by ablation of Zn bulk in distilled water at different LATs (5-20 min) at a set average power of 200 mW. Since ZnO has a higher absorbance [28] and a better reaction to UV light, its conductivity improves. This characteristic significantly increases the interaction with environmental (such as dyes) and biological (such as microbes) conditions [29, 30]. These metal nanoparticles have a fingerprint-like color in solutions. Surface plasmons, as defined by the Mie theory, are the collective oscillations of free electrons caused by the incident light's oscillating electromagnetic field plasmons [31]. Surface Plasmon Resonance (SPR) is about 245 nm. This figure indicates that an increase in LATs (5-20 min) for Zn bulk led to an increase in absorption peak intensity.

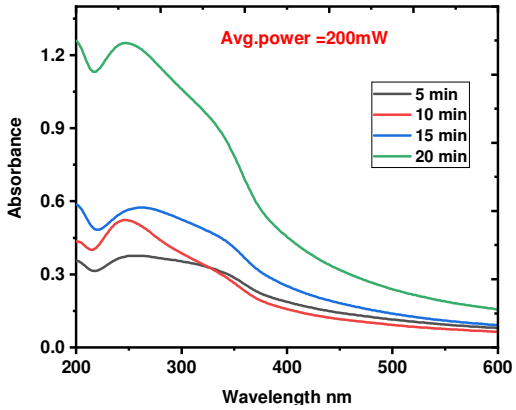

Fig. 3. Absorption spectrum for ZnO-NPs colloidal generated by PLAL.

B. Structure Characteristics

The ZnO-NPs were characterized in size and form utilizing a high-resolution transmission electron microscope (HR-TEM, JEM-2100, Joel, Japan, operated at 200 KV). To estimate the particle sizes of both ZnO-NPs, the colloidal samples were spread out on carbon-coated copper grids at room temperature and left to air dry. Using ImageJ software, the diameters of many dispersed particles in TEM pictures were measured [32]. Beyond that, a histogram was designed, and the average size of the NPs was ascertained using the Origin program. Figure 4 shows TEM images of ZnO-NPs, along with a chart with histograms of the size distribution. The analysis revealed that the NPs possessed a predominantly spherical morphology. The average size of ZnO-NPs varies with the different LATs (5-20 min) at a constant average power of 200 mW. The results indicate that increasing the LAT results in smaller average NP sizes, consistent with a laser-induced fragmentation mechanism, where average sizes were 32.3, 27.3, 23.02, and 20.6 nm at LATs of 5, 10, 15, and 20 min, respectively. According to the results, the synthesized product has a spherical structure and good distribution. The fragmentation mechanism concludes that the NPs get smaller as the LAT increases [33]. Figure 5 illustrates the inverse relationship between average ZnO-NP size and increasing LAT (5-20 min) at a constant laser power of 200 mW. This figure illustrates how LAT increased from 5 min to 20 min while average NPs sizes reduced from 32.3 nm to 20.6 nm. This reflects the fragmentation process where longer LAT leads to smaller NP size [34-36].

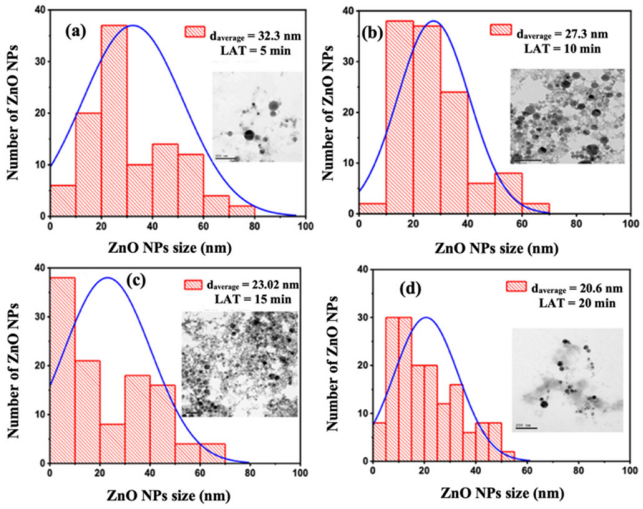

Fig. 4. Histogram of the average size of ZnO NPs with varying LATs, (a) 5 min, (b) 10 min, (c) 15 min, and (d) 20 min, at a constant average power of 200 mW. The insets of figures (a-d) indicate the shape of the NPs formed.

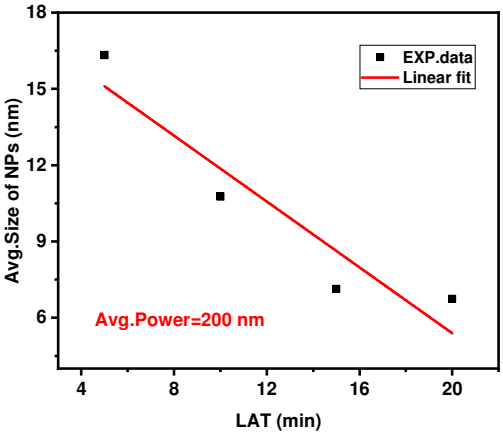

Fig. 5. The average size variation of ZnO-NPs with altering LATs (5-20 min) at a constant average power of 200 mW.

C. Concentration of ZnO-NPs

The concentration of ZnO-NPs prepared by PLAL was measured using an inductively coupled plasma device (Agilent

5100 Synchronous Vertical Dual View (SVDV) ICP–OES, Agilent Vapor Generation Accessory VGA 77). Figure 6 shows the impact of varying LATs on the concentration of colloidal ZnO-NPs. This figure indicates that as the LAT grew, the concentration of colloidal ZnO-NPs increased correspondingly. As shown in Figure 3, higher absorption intensities correlated with increased ZnO-NP concentrations, supporting the notion that longer LAT enhances NP yield. The concentration of ZnO-NPs increased progressively with LATs of 5, 10, 15, and 20 minutes, reaching values of 6.9, 13.3, 17.5, and 38.25 mg/L, respectively, under a constant average laser power of 200 mW.

ZnO-NPs suspended in distilled water reached a concentration of 38.25 mg/L when the exposed Zinc sample was exposed to a higher LAT of 20 min. This contrasts with the lower concentrations observed at shorter LATs, confirming that prolonged laser exposure promotes a higher ZnO-NP yield. Numerous biological activities are dependent on the Zn concentrations in the nanoscale region of NPs. The larger surface area and increased concentration are responsible for ZnO-NP applications [37-39].

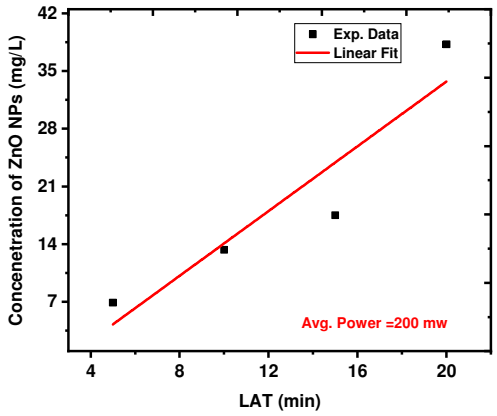

Fig. 6. Variation in ZnO-NP concentration with different LATs (5-20 min).

The physical characteristics of the ZnO-NPs, particularly particle size and concentration, showed a clear dependence on LAT. As LAT increased from 5 to 20 minutes, the average particle size decreased from 32.3 to 20.6 nm, while the NP concentration increased substantially (from 6.9 to 38.25 mg/L). These changes likely contributed to the enhanced cytotoxicity observed in A375 melanoma cells. As particle size decreases, the surface area-to-volume ratio increases, exposing more reactive sites capable of generating ROS upon laser irradiation. Similarly, higher NP concentrations raise the total available surface area for interaction with cellular components. Together, these factors potentiate oxidative stress and mitochondrial dysfunction in cancer cells, ultimately resulting in decreased viability. These observations support the hypothesis that the physical optimization of ZnO-NPs via laser ablation can directly enhance their biological effectiveness.

Figure 7 shows the EDX spectrum of the ZnO NPs. According to the EDX spectrum, ZnO NPs contain 90.07 % Zn and 9.93 % by weight. Thus, the presence of O and Zn in the produced substance was verified.

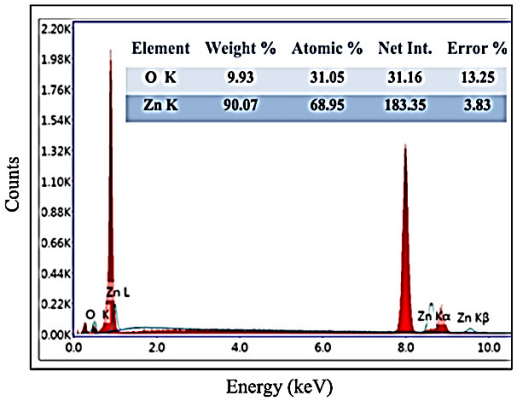

Fig. 7. EDX spectrum of ZnO-NPs colloidal solution prepared by PLAL.

D. Effect of Different Concentrations of ZnO-NPs on A375 Cells' Viability.

Compared to control cells, cell viability decreased to 32% at the maximum ZnO-NPs concentration of 15.3 µg/mL, which was statistically significant (***p<0.001), confirming the concentration-dependent cytotoxic potential of the NPs. However, as Figure 8 illustrates, there were no appreciable variations in cell survival between the control group and cells treated with lower concentrations of ZnO-NPs. In A375 cells, ZnO-NPs showed concentration-dependent cytotoxicity, which is in line with the results of [7]. This is also in agreement with [28], which demonstrated the effect of ZnO NPs on U251 cells.

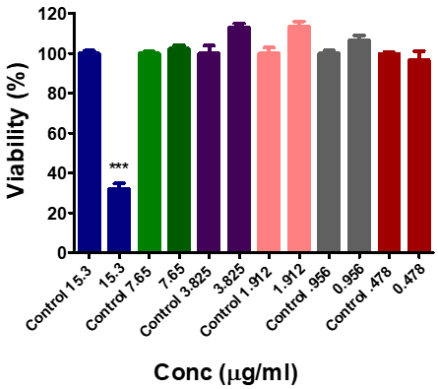

Fig. 8. The impact of ZnO-NPs on A375 cell viability 24 hours post-treatment. Cell viability was assessed using the MTT test and is shown as the proportion of untreated cells (control). Significant variation from the control, with ***p < 0.001.

E. Effect of Femtosecond Laser and ZnO-NPs on A375 Cells' Biability

The results of the MTT assay indicated that the viability of ocular melanoma cells, relative to the control, was 48% following femtosecond laser treatment at 420 nm, 32% with ZnO-NPs alone (15.3 µg/mL), and 1.3% with the combination of ZnO-NPs and femtosecond laser treatment at 420 nm, which was statistically significant compared to either treatment alone (***p<0.001), as shown in Figure 9. These findings confirm the potency of the synergistic treatment approach. The enhanced cytotoxic effect observed with the 420 nm

femtosecond laser in combination with ZnO-NPs can be attributed to the wavelength's proximity to the absorption band of ZnO-NPs, which peaks at 245 nm but exhibits a broad absorption tail extending into the visible range. The 420 nm wavelength likely excites the ZnO-NPs effectively, leading to the generation of ROS that induce oxidative stress and apoptotic cell death. This synergistic effect is evident in the drastic reduction of A375 cell viability to 1.3%, compared to 48% with 420 nm laser alone and 32% with ZnO-NPs alone.

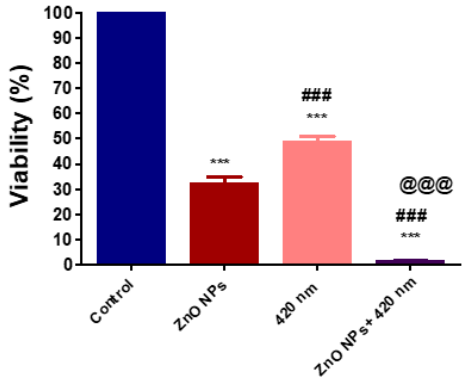

Fig. 9. The impact of ZnO-NPs and 420 nm femtosecond laser irradiation on A375 cell survival 24 hours post-treatment. Cell viability, expressed as the proportion of untreated cells (control), was assessed using the MTT test. Symbols indicate significant differences: *** indicates a significant difference compared to the control with $p<0.001$, ### denotes a significant difference observed compared to ZnO-NPs treatment with $p<0.001$, and @@@ signifies a significant difference observed compared to 420 nm treatment with $p<0.001$.

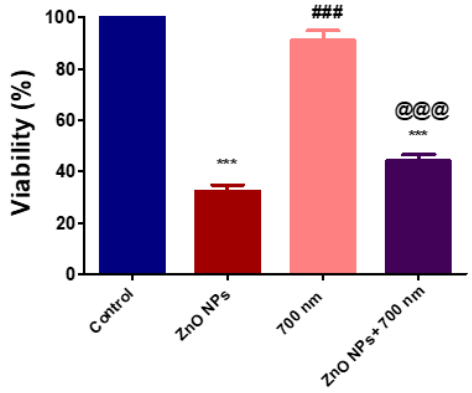

Fig. 10. The impact of ZnO-NPs and 700 nm femtosecond laser irradiation on A375 cell survival 24 hours post-treatment. Cell viability, which is expressed as the proportion of untreated cells (control), was assessed using the MTT test. Symbols indicate significant differences: *** indicates a significant difference compared to the control with $p<0.001$, ### denotes a significant difference observed compared to ZnO-NPs treatment with $p< 0.001$, and @@@ signifies a significant difference observed compared to 700 nm treatment with $p<0.001$.

In contrast, no significant difference in cell viability was observed between the control and cells treated with the femtosecond laser at 700 nm. These findings align with those of [40], which reported that irradiation of T47D breast cancer cells with a femtosecond laser at 420 nm had a significant impact, whereas no effect was observed at 700 nm. Additionally, as shown in Figure 10, no significant difference was observed between the effects of ZnO-NPs alone and the combination of ZnO-NPs with femtosecond laser treatment at 700 nm, reinforcing the wavelength specificity of the observed cytotoxic effects. This outcome may be attributed to the fact that 700 nm is far from the absorption spectrum of ZnO-NPs, which peaks at 245 nm, resulting in insufficient photon absorption and minimal ROS production. This wavelength specificity highlights the importance of tuning the laser source to match the photophysical properties of the nanoparticles in order to optimize therapeutic efficacy.

IV. CONCLUSIONS

This study addressed a significant therapeutic challenge in ocular melanoma by exploring a novel combinatorial strategy involving ZnO-NPs synthesized through PLAL and their synergistic cytotoxicity with femtosecond laser light. Conventional treatments often suffer from non-specificity and toxicity, highlighting the need for innovative and targeted approaches. ZnO-NPs were synthesized using a clean, surfactant-free PLAL method, ensuring high purity and optimal biocompatibility. Their characterization revealed a decreasing NP size with increasing LAT, with an average size of 20.6 nm at 20 minutes LAT. Subsequent biological assays demonstrated that ZnO-NPs alone reduced the viability of A375 ocular melanoma cells to 32%, while femtosecond laser exposure at 420 nm achieved 48% viability. Notably, the combination of ZnO-NPs and 420 nm femtosecond irradiation reduced cell viability drastically to 1.3%, demonstrating a powerful synergistic effect. In contrast, 700 nm laser exposure showed negligible cytotoxicity, indicating wavelength specificity linked to ZnO-NPs absorption properties.

To the best of our knowledge, this is the first study demonstrating such enhanced melanoma cell suppression through femtosecond irradiation combined with laser-synthesized ZnO-NPs. Although the results are promising, this study was conducted in vitro and lacks long-term biocompatibility and safety evaluations. In addition, potential effects on surrounding healthy ocular tissues must be carefully assessed. Future investigations will focus on in vivo validation, mechanistic studies of intracellular ROS pathways, and the development of targeted delivery systems to advance this technique toward clinical application in ocular oncology.

REFERENCES

[1] H. Y. Tsai *et al.*, "Machine Learning Algorithms for ccRCC Data Analysis," in *2022 IEEE 4th Eurasia Conference on Biomedical Engineering, Healthcare and Sustainability (ECBIOS)*, Tainan, Taiwan, May 2022, pp. 203–206, https://doi.org/10.1109/ECBIOS54627.2022.9945034.

[2] M. S. Goldberg, J. T. Doucette, H. W. Lim, J. Spencer, J. A. Carucci, and D. S. Rigel, "Risk factors for presumptive melanoma in skin cancer screening: American Academy of Dermatology National Melanoma/Skin Cancer Screening Program experience 2001-2005," *Journal of the American Academy of Dermatology*, vol. 57, no. 1, pp. 60–66, Jul. 2007, https://doi.org/10.1016/j.jaad.2007.02.010.

[3] T. Marugame and M. J. Zhang, "Comparison of Time Trends in Melanoma of Skin Cancer Mortality (1990–2006) Between Countries Based on the WHO Mortality Database," *Japanese Journal of Clinical Oncology*, vol. 40, no. 7, Jul. 2010, Art. no. 710, https://doi.org/10.1093/jjco/hyq107.

[4] A. Stratigos *et al.*, "Melanoma/skin cancer screening in a Mediterranean country: results of the Euromelanoma Screening Day Campaign in Greece," *Journal of the European Academy of Dermatology and Venereology*, vol. 21, no. 1, pp. 56–62, 2007, https://doi.org/10.1111/j.1468-3083.2006.01865.x.

[5] W. Sun and L. M. Schuchter, "Metastatic melanoma," *Current Treatment Options in Oncology*, vol. 2, no. 3, pp. 193–202, Jun. 2001, https://doi.org/10.1007/s11864-001-0033-5.

[6] M. Batus, S. Waheed, C. Ruby, L. Petersen, S. D. Bines, and H. L. Kaufman, "Optimal Management of Metastatic Melanoma: Current Strategies and Future Directions," *American Journal of Clinical Dermatology*, vol. 14, no. 3, pp. 179–194, Jun. 2013, https://doi.org/10.1007/s40257-013-0025-9.

[7] R. Parthasarathy, R. Ramachandran, Y. Kamaraj, and S. Dhayalan, "Zinc Oxide Nanoparticles Synthesized by Bacillus cereus PMSS-1 Induces Oxidative Stress-Mediated Apoptosis via Modulating Apoptotic Proteins in Human Melanoma A375 Cells," *Journal of Cluster Science*, vol. 33, no. 1, pp. 17–28, Jan. 2022, https://doi.org/10.1007/s10876-020-01941-1.

[8] M. A. Postow, J. Harding, and J. D. Wolchok, "Targeting Immune Checkpoints: Releasing the Restraints on Anti-Tumor Immunity for Patients With Melanoma," *The Cancer Journal*, vol. 18, no. 2, Apr. 2012, Art. no. 153, https://doi.org/10.1097/01.PPO.0000581876.62921.87.

[9] K. Guidolin and G. Zheng, "Nanomedicines Lost in Translation," *ACS Nano*, vol. 13, no. 12, pp. 13620–13626, Dec. 2019, https://doi.org/10.1021/acsnano.9b08659.

[10] D. Gal, G. Hodes, D. Lincot, and H. W. Schock, "Electrochemical deposition of zinc oxide films from non-aqueous solution: a new buffer/window process for thin film solar cells," *Thin Solid Films*, vol. 361–362, pp. 79–83, Feb. 2000, https://doi.org/10.1016/S0040-6090(99)00772-5.

[11] J. Shi, Q. Cao, Y. Wei, and Y. Huang, "ZnO varistor manufactured by composite nano-additives," *Materials Science and Engineering: B*, vol. 99, no. 1, pp. 344–347, May 2003, https://doi.org/10.1016/S0921-5107(02)00492-0.

[12] S. Bai, X. Liu, D. Li, S. Chen, R. Luo, and A. Chen, "Synthesis of ZnO nanorods and its application in NO2 sensors," *Sensors and Actuators B: Chemical*, vol. 153, no. 1, pp. 110–116, Mar. 2011, https://doi.org/10.1016/j.snb.2010.10.010.

[13] Z. L. Wang, "Ten years' venturing in ZnO nanostructures: from discovery to scientific understanding and to technology applications," *Chinese Science Bulletin*, vol. 54, no. 22, pp. 4021–4034, Nov. 2009, https://doi.org/10.1007/s11434-009-0456-0.

[14] Y. Tu *et al.*, "Transparent and flexible thin films of ZnO-polystyrene nanocomposite for UV-shielding applications," *Journal of Materials Chemistry*, vol. 20, no. 8, pp. 1594–1599, Feb. 2010, https://doi.org/10.1039/B914156A.

[15] N. Saito, H. Haneda, T. Sekiguchi, N. Ohashi, I. Sakaguchi, and K. Koumoto, "Low-Temperature Fabrication of Light-Emitting Zinc Oxide Micropatterns Using Self-Assembled Monolayers," *Advanced Materials*, vol. 14, no. 6, pp. 418–421, 2002, https://doi.org/10.1002/1521-4095(20020318)14:6<418::AID-ADMA418>3.0.CO;2-K.

[16] P. Katangur, P. K. Patra, and S. B. Warner, "Nanostructured ultraviolet resistant polymer coatings," *Polymer Degradation and Stability*, vol. 91, no. 10, pp. 2437–2442, Oct. 2006, https://doi.org/10.1016/j.polymdegradstab.2006.03.018.

[17] A. Mir, N. Becheikh, L. Khezami, M. Bououdina, and A. Ouderni, "Synthesis, Characterization, and Study of the Photocatalytic Activity upon Polymeric-Surface Modification of ZnO Nanoparticles," *Engineering, Technology & Applied Science Research*, vol. 13, no. 6, pp. 12047–12053, Dec. 2023, https://doi.org/10.48084/etasr.6373.

[18] A. G. Schiopu *et al.*, "Characterization of Pure and Doped ZnO Nanostructured Powders elaborated in Solar Reactor," *Engineering, Technology & Applied Science Research*, vol. 14, no. 2, pp. 13502–13510, Apr. 2024, https://doi.org/10.48084/etasr.6923.

[19] C. Hanley *et al.*, "Preferential killing of cancer cells and activated human T cells using ZnO nanoparticles," *Nanotechnology*, vol. 19, no. 29, Mar. 2008, Art. no. 295103, https://doi.org/10.1088/0957-4484/19/29/295103.

[20] J. W. Rasmussen, E. Martinez, P. Louka, and D. G. Wingett, "Zinc oxide nanoparticles for selective destruction of tumor cells and potential for drug delivery applications," *Expert Opinion on Drug Delivery*, vol. 7, no. 9, pp. 1063–1077, Sep. 2010, https://doi.org/10.1517/17425247.2010.502560.

[21] P. M. Aneesh, K. A. Vanaja, and M. K. Jayaraj, "Synthesis of ZnO nanoparticles by hydrothermal method," presented at the NanoScience + Engineering, San Diego, CA, USA, Sep. 2007, Art. no. 66390J, https://doi.org/10.1117/12.730364.

[22] T. S. Ko *et al.*, "ZnO nanopowders fabricated by dc thermal plasma synthesis," *Materials Science and Engineering: B*, vol. 134, no. 1, pp. 54–58, Sep. 2006, https://doi.org/10.1016/j.mseb.2006.07.019.

[23] S. Jurablu, M. Farahmandjou, and T. P. Firoozabadi, "Sol-Gel Synthesis of Zinc Oxide (ZnO) Nanoparticles: Study of Structural and Optical Properties," *Journal of Sciences, Islamic Republic of Iran*, vol. 26, no. 3, pp. 281–285, Sep. 2015.

[24] H. Huang, J. Lai, J. Lu, and Z. Li, "Pulsed laser ablation of bulk target and particle products in liquid for nanomaterial fabrication," *AIP Advances*, vol. 9, no. 1, Jan. 2019, Art. no. 015307, https://doi.org/10.1063/1.5082695.

[25] T. Mohamed, A. Farhan, H. Ahmed, M. Ashour, S. Mamdouh, and R. Schuch, "Nonlinear Optical Properties of Zinc Oxide Nanoparticle Colloids Prepared by Pulsed Laser Ablation in Distilled Water," *Nanomaterials*, vol. 12, no. 23, Jan. 2022, Art. no. 4220, https://doi.org/10.3390/nano12234220.

[26] E. Fazio *et al.*, "Nanoparticles Engineering by Pulsed Laser Ablation in Liquids: Concepts and Applications," *Nanomaterials*, vol. 10, no. 11, Nov. 2020, Art. no. 2317, https://doi.org/10.3390/nano10112317.

[27] C. A. Perez-Lopez, J. A. Perez-Taborda, H. Riascos, and A. Avila, "The influence of pulsed laser ablation in liquids parameters on the synthesis of ZnO nanoparticles," *Journal of Physics: Conference Series*, vol. 1541, no. 1, Mar. 2020, Art. no. 012019, https://doi.org/10.1088/1742-6596/1541/1/012019.

[28] H. M. Xiong, "ZnO Nanoparticles Applied to Bioimaging and Drug Delivery," *Advanced Materials*, vol. 25, no. 37, pp. 5329–5335, 2013, https://doi.org/10.1002/adma.201301732.

[29] R. Wahab *et al.*, "Low temperature solution synthesis and characterization of ZnO nano-flowers," *Materials Research Bulletin*, vol. 42, no. 9, pp. 1640–1648, Sep. 2007, https://doi.org/10.1016/j.materresbull.2006.11.035.

[30] Ü. Özgür *et al.*, "A comprehensive review of ZnO materials and devices," *Journal of Applied Physics*, vol. 98, no. 4, Aug. 2005, Art. no. 041301, https://doi.org/10.1063/1.1992666.

[31] P. Mulvaney, "Surface Plasmon Spectroscopy of Nanosized Metal Particles," *Langmuir*, vol. 12, no. 3, pp. 788–800, Jan. 1996, https://doi.org/10.1021/la9502711.

[32] A. Neumeister, J. Jakobi, C. Rehbock, J. Moysig, and S. Barcikowski, "Monophasic ligand-free alloy nanoparticle synthesis determinants during pulsed laser ablation of bulk alloy and consolidated microparticles in water," *Physical Chemistry Chemical Physics*, vol. 16, no. 43, pp. 23671–23678, 2014, https://doi.org/10.1039/C4CP03316G.

[33] G. Bongiovanni, P. K. Olshin, C. Yan, J. M. Voss, M. Drabbels, and U. J. Lorenz, "The fragmentation mechanism of gold nanoparticles in water under femtosecond laser irradiation," *Nanoscale Advances*, vol. 3, no. 18, pp. 5277–5283, 2021, https://doi.org/10.1039/D1NA00406A.

[34] A. O. El-Gendy, A. Samir, E. Ahmed, C. S. Enwemeka, and T. Mohamed, "The antimicrobial effect of 400 nm femtosecond laser and silver nanoparticles on gram-positive and gram-negative bacteria," *Journal of Photochemistry and Photobiology B: Biology*, vol. 223, Oct. 2021, Art. no. 112300, https://doi.org/10.1016/j.jphotobiol.2021.112300.

[35] J. Zhang and C. Q. Lan, "Nickel and cobalt nanoparticles produced by laser ablation of solids in organic solution," *Materials Letters*, vol. 62, no. 10, pp. 1521–1524, Apr. 2008, https://doi.org/10.1016/j.matlet.2007.09.038.

[36] S. Mamdouh, A. Mahmoud, A. Samir, M. Mobarak, and T. Mohamed, "Using femtosecond laser pulses to investigate the nonlinear optical properties of silver nanoparticles colloids in distilled water synthesized

by laser ablation," *Physica B: Condensed Matter*, vol. 631, Apr. 2022, Art. no. 413727, https://doi.org/10.1016/j.physb.2022.413727.

[37] A. Ashrafi and C. Jagadish, "Review of zincblende ZnO: Stability of metastable ZnO phases," *Journal of Applied Physics*, vol. 102, no. 7, Oct. 2007, Art. no. 071101, https://doi.org/10.1063/1.2787957.

[38] R. Aghababazadeh, B. Mazinani, A. Mirhabibi, and M. Tamizifar, "ZnO Nanoparticles Synthesised by mechanochemical processing," *Journal of Physics: Conference Series*, vol. 26, no. 1, Oct. 2006, Art. no. 312, https://doi.org/10.1088/1742-6596/26/1/075.

[39] A. Umamaheswari, P. S. Lakshmana, and A. Puratchikody, "Biosynthesis of zinc oxide nanoparticle: a review on greener approach," *MOJ Bioequivalence & Bioavailability*, vol. 5, no. 3, Jun. 2018, https://doi.org/10.15406/mojbb.2018.05.00096.

[40] S. Taha, W. R. Mohamed, M. A. Elhemely, A. O. El-Gendy, and T. Mohamed, "Tunable femtosecond laser suppresses the proliferation of breast cancer *in vitro*," *Journal of Photochemistry and Photobiology B: Biology*, vol. 240, Mar. 2023, Art. no. 112665, https://doi.org/10.1016/j.jphotobiol.2023.112665.